Avrupa Bilim ve Teknoloji Dergisi
Sayı 41, S. 23-30, Kasım 2022

Araştırma Makalesi

www.ejosat.com ISSN:2148-2683

European Journal of Science and Technology
No. 41, pp. 23-30, November 2022

Research Article

Effect of Magnetohydrodynamic Second Order Slip Flow Boundary Condition Coefficients on Flow in Parallel Plates

Hatice Şimşek[1*]

[1*] Tekirdag Namik Kemal University, Vocational School of Technical Sciences, Tekirdag, Turkey, (ORCID: 0000-0003-0041-3406), h.simsek@nku.edu.tr

(First received 25 March 2022 and in final form 2 May 2022)

(**DOI:** 10.31590/ejosat.)

ATIF/REFERENCE: Şimşek, H. (2022). Effect of Magnetohydrodynamic Second Order Slip Flow Boundary Condition Coefficients on Flow in Parallel Plates. *Avrupa Bilim ve Teknoloji Dergisi*, (41), 23-30.

Abstract

In this study, the fully developed velocity profile in magnetohydrodynamic (MHD) flow between microparallel plates was analyzed analytically using all the second-order slipvelocity boundary conditions available in the literature. The heat flux is assumed to be constant. The magnetic field acts perpendicular to the plate surface. The momentum equation is solved analytically using the quadratic slip velocity boundary condition model in slip flow. The extent to which the second-order slip velocity boundary conditions affect the slip flow at the center and at the wall is shown with both graphs and tables. In the study, it was emphasized how effective the magnetic field is especially in the case of second order slip flow, and the percentage of the second order slip flow in the presence/absence of magnetic field was calculated as a percentage.

Keywords: MHD, Second order velocity slip, Parallel plate, Viscous dissipation, Analytical solution

[*] Corresponding Author: h.simsek@nku.edu.tr

1. Introduction

In the 1980s, MEMS (micro-electro-mechanical systems), a new field covering all aspects of science and technology, has become the focus of attention of many researchers.

Magneto-hydrodynamics (MHD) plays a very significant role in astrophysics, galactic magnetism, engineering, and controlled nuclear fusion. As in nature, the magnetic field or MHD affects the behaviour of fluid and flow in industrial processes. In addition to micro electronic industry, medical industry, micro-device technology, bioengineering and micro-scale heat exchanger systems, simultaneous increase of technical applications at micro-scale level in aviation, food, chemical, pharmaceutical and automotive industries has led to a recent growth of importance for fluids to determine the momentum and heat transfer characteristics in magneto-hydrodynamics (MHD) flow at micro-scale. The electrically conductive fluid is affected by the magnetic field both in terms of heat transfer and flow. This makes magnetic field important as a heat transfer recovery method.

With increasing dilution and dilution in the gas flow in microchannels, more accurate boundary conditions were required and a second-order slip velocity boundary condition was used. The absence of a conventionally accepted second-order slip boundary condition in the literature makes it difficult to use the slip flow equations. Despite the studies, uncertainties remain on the correct value of the second-order slip boundary condition coefficient. Undoubtedly, in this case, it emerges as an important problem extending to the Navier-Stokes equations in the transition flow regime.

In the study, the second order slip velocity boundary condition coefficients proposed by [1], [2], [3], [4], [5], [6], [7], [8], [9],[10] how it affects the slip velocity was investigated.

The extent to which MHD flow affects heat transfer and flow control was investigated for the first time by [11]. Depending on the electrical conductivity and magnetization property, the flow rates and speeds of fluids vary under the impact of a magnetic field. If a magnetic field is applied to a fluid with electrical conductivity, an electric current is induced in the fluid, and the so-called Lorentz force is formed between the resulting electric current and the magnetic field. Thus, emerging Lorentz force affects the fluid flow, hence heat transfer. The generation of these currents has also led to designing appliances such as MHD generator devices, MHD pumps, accelerators and flow-meters.

In the literature where the second-order velocity boundary conditions model for slip flow government was used for different geometries, either merely slip flow regime or magneto-hydrodynamics (MHD) was taken into account simultaneously with slip flow regime. Those studies are summarized below.

The fully developed gas flow between parallel plates is investigated in the work by [12] and the momentum and energy equations are solved using both the slip flow and temperature jump boundary conditions of the second order. In his work, [13] has obtained the second-order slip boundary condition model from the Kinetics Theory for the wall-bounded dilution (rarefied) gas flow. The slip flow contains very close estimates to numerical solutions of linearised Boltzmann equation for entire Knudsen numbers. [14] have analysed the viscous fluid flow and heat transfer through an isothermal, pervious and linear shrinking plate that was exposed to constant absorption and placed in a stagnant medium, by using the second-order slip flow model previously proposed by [13]. [15] has numerically studied some basic parameters of fluid flow and heat transfer including slip coefficient, magnetic parameter, Prandtl Nu with Eckert Nu and the impact of viscous dissipation on the slip flow of electrically conductive fluid moving through a permeable surface in two-dimensional and steady regime. [16] has experimentally examined gas flow through a rectangular micro-channel using the second-order slip boundary condition whereas [17] has numeriacally investigated the slip flow in a natural convection by applying constant heat flux to the walls of a micro channel with perpendicular parallel plates. Stagnation point flow from a vertical plate with constant heat flux, in mixed convection under a steady regime has been discussed by [18] using the second-order slip flow model proposed by [13] whereas [19] have examined heat transfer through a vertical, porous and expanding / shrinking plate under a permanent regime referring to the same model by [13]. The MHD was analyzed analytically by study [20] on how the second-order slip flow affects heat and mass transfer. In the study, MHD flow and heat transfer over a permeable expanding/shrinking surface was discussed using the second-order slip model. Another research by [21] has examined the heat transfer of frictional Maxwell flow over MHD flow on a porous medium while analysing the second order slip effect as well. [22] have analysed the effect of second-order slip on the flow of a Maxwell fluid with second-order friction while monitoring the second-order slip flow between the wall and the fluid on it. [23] have investigated the effect of magnetic field and second-order slip flow on kasson flow through heat transfer, which is subject to suction/injection and convective boundary condition. Their analyses have depicted that friction on the surface was increased by the progress of the second-order slip parameter, in the existence of kasson flow parameter and Nusselt number. [24] have theoretically discussed the combined analysis of entropy generation and activation energy via modeling the second-order slip velocity flow on a sloping parabolized surface.[25] have monitored the MHD flow of nanofluids creating homogeneous-heterogeneous reaction on a porous medium, influenced by the second-order slip velocity. Under these conditions, the basic flow equation has been entirely solved and the coefficient of surface friction has been found to be significantly different from the results of previous literature, in the presence of second order slip rates. Another research by [26] has focused on joule heating, and second-order the distributor flow at MHD stagnation on a permeable medium with joule heating and second order slip condition. They have numerically and graphically modelled the effects of viscous diffusion, Joule heating and the second-order slip on flow area by comparing various values of the basic parameters.

Generally, the second-order slip velocity boundary conditions are it is shown in equation (1).

$$\mathrm{u_s} - \mathrm{u_w} = b_1 \lambda \left.\frac{\partial \mathrm{u}}{\partial \mathrm{y}}\right|_{\mathrm{w}} - b_2 \lambda^2 \left.\frac{\partial^2 \mathrm{u}}{\partial \mathrm{y}^2}\right|_{\mathrm{w}}, \qquad (1)$$

are explained by this model. Here us slip velocity, uw wall speed, b_1 first order slip velocity boundary condition coefficients, b_2 second order slip velocity boundary condition coefficents, respectively.

Table 1. b_1 and b_2 Slip velocity boundary condition coefficients

Author	b_1	b_2
Cercignani and Daneri, (1963)	1.1466	0.9756
Cercignani & Lorenzani, (2010)	1.1209	0.2347
Deissler, (1964)	1	9/8
Hadjiconstantinou, (2003)	1.11	0.61
Hsia and Domoto, (1983)	1	1/2
Karniadakis & Beskok, (2002)	1	-1/2
Lorenzani, (2011)	1.1366	0.69261
Mitsuya, (1993)	1	2/9
Pitakarnnop et al., (2010)	1.1466	0.647
Schamberg, (1947)	1	$5\pi/12$

This study demonstrates ten models proposed by [1], [2], [3], [4], [5], [6], [7], [8], [9], and [10] with authors' names and the corresponding coefficients for each model, as tabulated in table 1.

The aim of this study is to reveal the extent to which the coefficients of the second-order slip velocity boundary conditions existing in the literature, when used together with the magnetic parameter ¨M¨, affect the velocity profiles in the slip flow.

2. Material and Method

2.1. Formulation Of The Problem

The geometry and coordinate system is displayed in Figure 1. The magnetic Reynolds number is small and has been neglected next to the magnetic field induced by the motion of the electrically conductive fluid. At the same time, electric field strength, Hall effect and Joule heating are neglected. The flow is two-dimensional and the coordinate system is placed in the center of the microplates. The x-axis is placed on the center axis and the y-axis is perpendicular to it. Under these conditions, the basic dimensional equations of the flow under the influence of magnetic field, conservation of mass and conservation of momentum and its equation are given below.

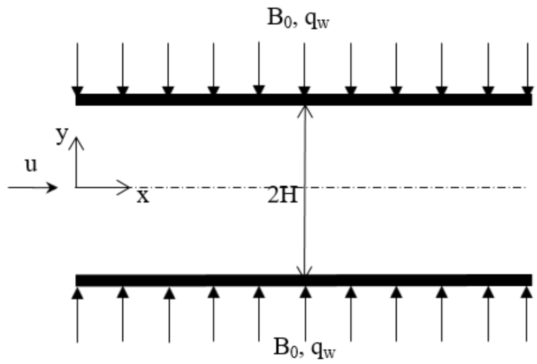

Figure 1. Geometry and coordinate system.

Regarding the above assumption, equation (2) is momentum equation, equations (3) and (4) define the quadratic slip velocity boundary conditions;

$$\frac{d^2u}{dy^2} = \frac{1}{\mu}\frac{dp}{dx} + \frac{\sigma B_0^2}{\mu}u, \quad (2)$$

$$y = 0, \qquad \left.\frac{\partial u}{\partial y}\right|_{y=0} = 0\,, \quad (3)$$

$$y = +H, \qquad u = u_s = -b_1\lambda\left.\frac{\partial u}{\partial y}\right|_{y=+H} - b_2\lambda^2\left.\frac{\partial^2 u}{\partial y^2}\right|_{y=+H} \quad (4)$$

where σ, p, μ, B_0 represent electrical conductivity, pressure, dynamic viscosity and magnetic field strength of the fluid, respectively. Defining directly, us is the slip velocity, and λ symbolizes molecular mean free path.

Dimensionless quantities used in the analysis of the physical phenomenon examined in the study

$$X = \frac{x}{H}\,, \quad Y = \frac{y}{H}\,, \quad U = \frac{u}{u_m}\,, \quad U_s = \frac{u_s}{u_m}\,, \quad P = \frac{pH}{\mu u_m}, \quad (5)$$

It is defined as U dimensionless axial coordinate, dimensionless velocity component in X direction, um dimension average velocity, Us dimensionless sliding velocity, H half distance between plates, Y dimensionless normal coordinate, P dimensionless static pressure.

Dimensionless momentum equation in the X direction and coupled boundary conditions;

$$\frac{d^2U}{\partial Y^2} = \frac{dP}{dX} + M^2U\,, \quad (6)$$

$$Y = 0, \qquad \left.\frac{dU}{dY}\right|_{Y=0} = 0\,, \quad (7)$$

$$Y = 1, \qquad U = U_s = -2b_1Kn\left.\frac{dU}{dY}\right|_{Y=1} - 4b_2Kn^2\left.\frac{d^2U}{dY^2}\right|_{Y=1}, \quad (8)$$

M is the Hartmann number described by the Eq. (5)

$$M = \left(\frac{\sigma B_0^2 H^2}{\mu}\right)^{\frac{1}{2}}, \quad (9)$$

The analytical solution of Eq. (6) which is dependent to the boundary conditions in Eqs. (7-8) is achieved;

$$U = \frac{\zeta_1}{\zeta_2}, \quad (10)$$

$$\zeta_1 = M\,Cosh(MY) - M\,Cosh(M) - 2b_1KnM^2Sinh(M) - 4b_2Kn^2M^3Cosh(M), \quad (11)$$

$$\zeta_2 = Sinh(M) - MCosh(M) - 2b_1KnM^2\,Sinh(M) - 4b_2Kn^2M^3Cosh(M), \quad (12)$$

3. Results and Discussion

In this study, the results obtained for Knudsen numbers range from 0 to 0.1, while for Hartmann numbers it is between 0 and 2.

The impact of first, second order slip boundary condition model on the velocity field is displayed via different slip models, as shown in Figures 2-4, concerning the variations of Kn number, the basic parameter of slip flow, and M, the basic parameter of magnetic field.

Figure 2 exhibits the effect of first and second order slip boundary condition on velocity profile in various slip models, in the absence of magnetic field influence (M= 0). At M = 0 and Kn = 0, non-sliding state occurs on the wall and axis with the first and second order slip boundary condition models. At M = 0, compared to the first order slip boundary condition, as the Knudsen number is increased by the second order slip boundary condition, slip velocity on the plate wall also rises for all models except Model [6] while a lowered effect is seen in axis velocity (maximum velocity) varying by the mass position. In Model [6], checked to the first order, the second order slip boundary condition for M= 0 decreases slip velocity on the plate wall with an increase in Kn number while enhancing the velocity on axis (highest velocity) in accordance with mass positioning.

The effect of magnetic field on velocity profile is shown in Figure 3 and Figure 4. Furthermore, slip velocity on the wall is much more increased by arising Knudsen number and magnetic field parameter M in a contradictory effect to the reduced axis velocity. The second order slip boundary condition accentuates this effect even more for all models excluding the Model [6] while making velocity profile more massive (flattened) and causing a larger increase in velocity on the wall than does the first order slip velocity boundary condition. In Model [6], an opposing situation is observed. Here, the second order slip boundary condition model is seen to lower slip velocity on the wall while raising it on the axis, depending on an rise in magnetic field parameter and Knudsen number.

In Figure 2-4, the dimensionless velocities intersect at the same point against the Knudsen number and the slip boundary condition model. This port indicates where the fluid velocity is equal to the medium velocity (U=1). Due to the suppression of the velocity profiles by the magnetic parameter M, the intersection point moves away from the axis and approaches the wall surface.

The utilization of second order slip boundary condition model is found out to increase velocity by 8.609% on the wall and decrease it by 1.714% on the axis for model [1] at M = 0, Kn = 0.1. The increase rate for model [2] is 2.402% on the wall the decrease on the axis is 0.378% ; for model [3], similar trends are detected as 11.473% increase on the wall and 1.886% decrease on axis. The results obtained for proceeding models are as follows: 5.929% increase on wall velocity and 0.978% decrease on axis for model [4]; 5.684% increase on the wall and 0.868% decrease on axis for model [5]; 6.959% decrease on wall velocity and 0.920% increase on axis velocity for model [6]; an increase of 6.459% on the wall and a decrease of 1.090% on the axis for model [7], an increase of 2.647% on the wall whereas a decrease of 0.390% on the axis for model [8], an increase of 5.996% on wall velocity whereas 1.013% decrease on axis velocity for model [9] and finally increasing rate of 12.972% on the wall with a decrescent impact on the axis by 2.171% model [10].

This variation is triggered by arising magnetic field impact so as to generate a velocity change at M = 2, Kn = 0.1 with the following scores: An increase by 14.069% on the wall and decrease by 2.638% on the axis for model [1], 4.352% increase on the wall and 0.705% decrease on the axis for model [2]; 11.473% velocity increase on the wall and 1.886% decrease on the axis for model [3] with no change at M = 0 and M = 2. The values appear as 10.164% increase on the wall and 1.764% decrease on the axis for model [4]; 9.843% increase on the wall and1.598% decrease on the axis for model [5]; 15.00% decrease on the wall whereas 1.837% increase on the axis for model [6], 10.940% increase on the wall and 1.954% decrease on the axis for model [7]; an increase of 4.838% in wall velocity whereas a decrease of 0.739% in axis velocity for model [8]; an increase in wall velocity by 10.233% with a decreasing value of 1.819% on the axis model for model [9], an increase on the wall by 20.162% whereas a decreasing velocity of 3.767% on the axis for model [10].

For models [1,2,4,5,7-10], the magnetic field fosters a reducing effect on wall slip velocity whereas an enhancing impact on the axis. The magnetic field is remarked to bring out a reverse situation for model [6] with an increasing slip velocity on the axis and decrescent one on the wall. Yet, no change is noted for model [3].

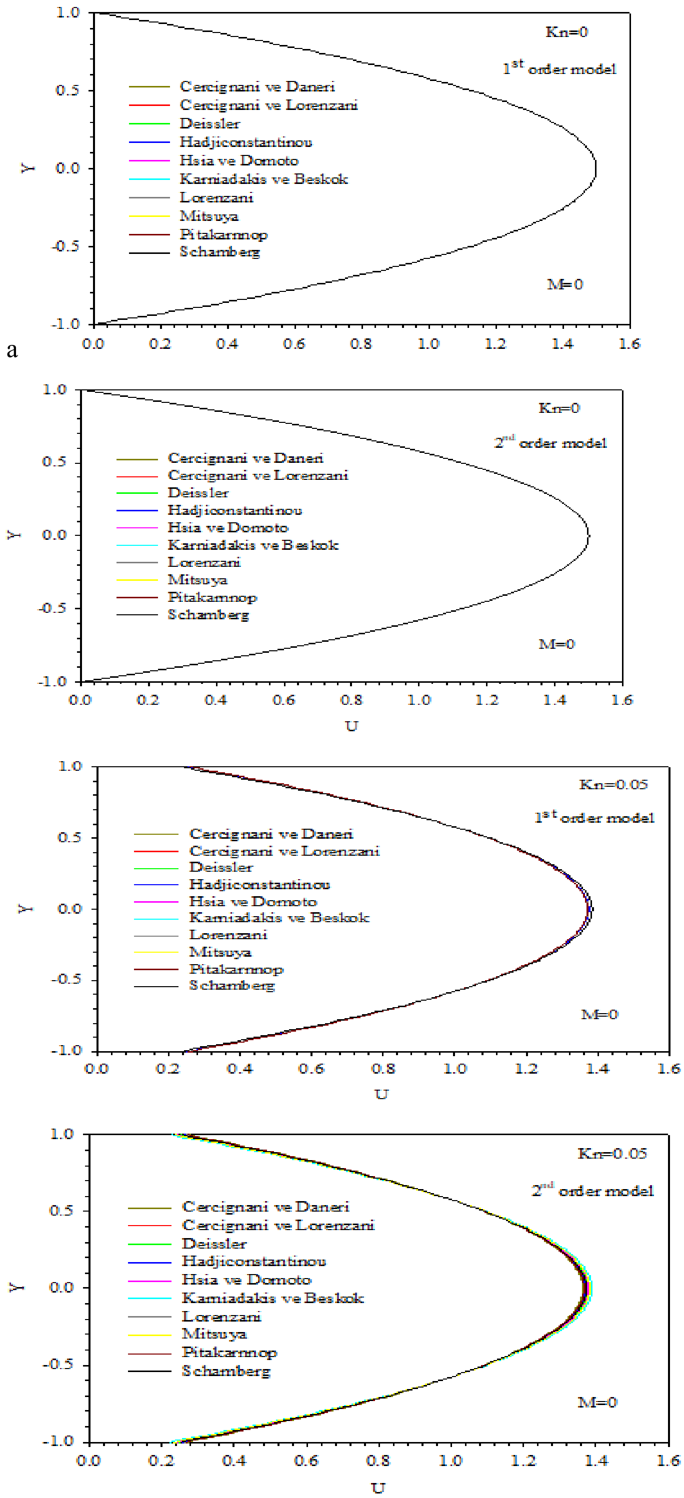

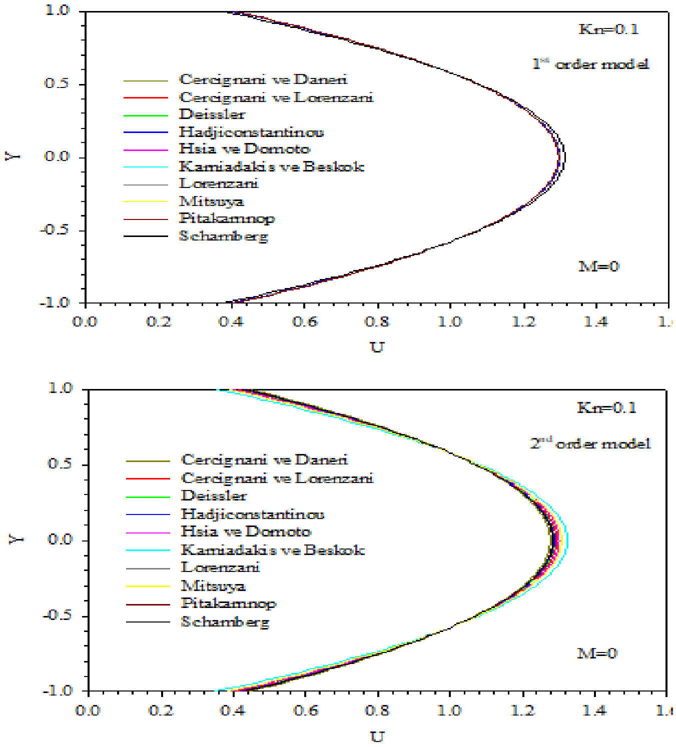

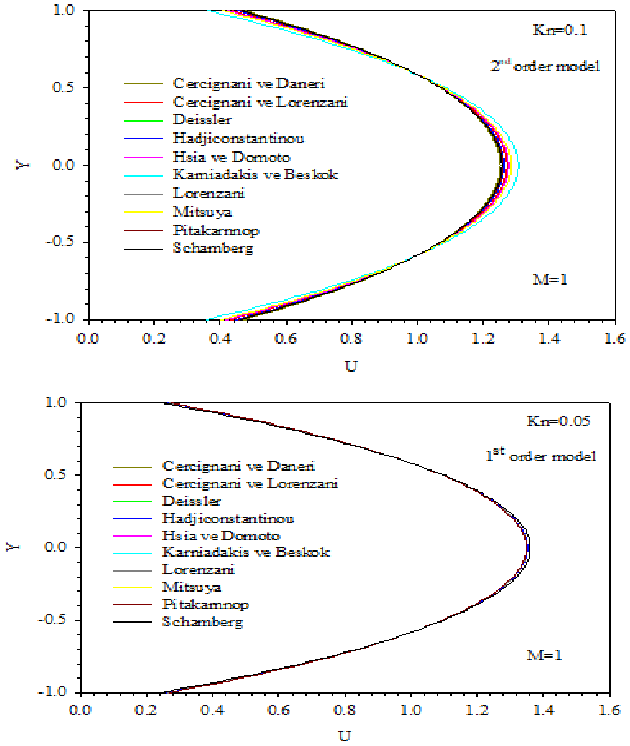

Figure 2. The impact of second order slip boundary conditions coefficient for various slip models on fully developed velocity profile (M= 0).

Figure 3. The impact of second order slip boundary conditions coefficient model for various slip models on fully developed velocity profile (M= 1).

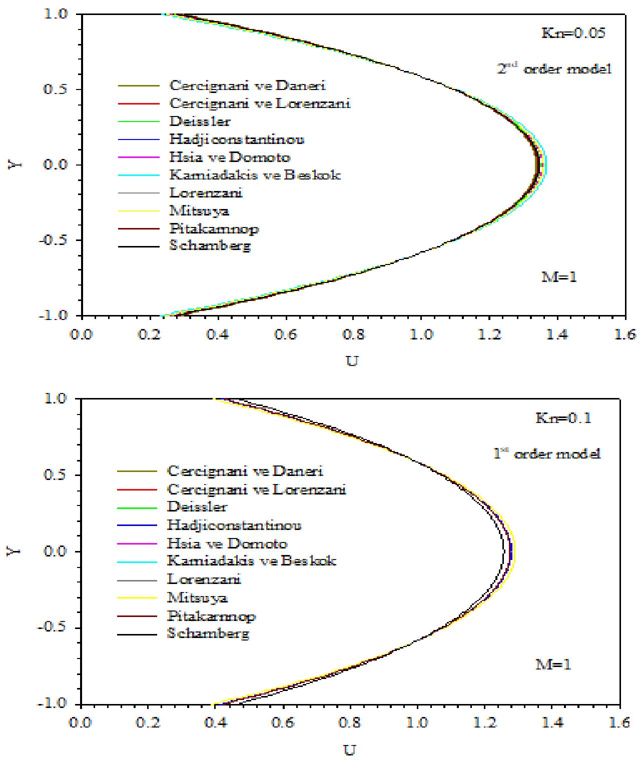

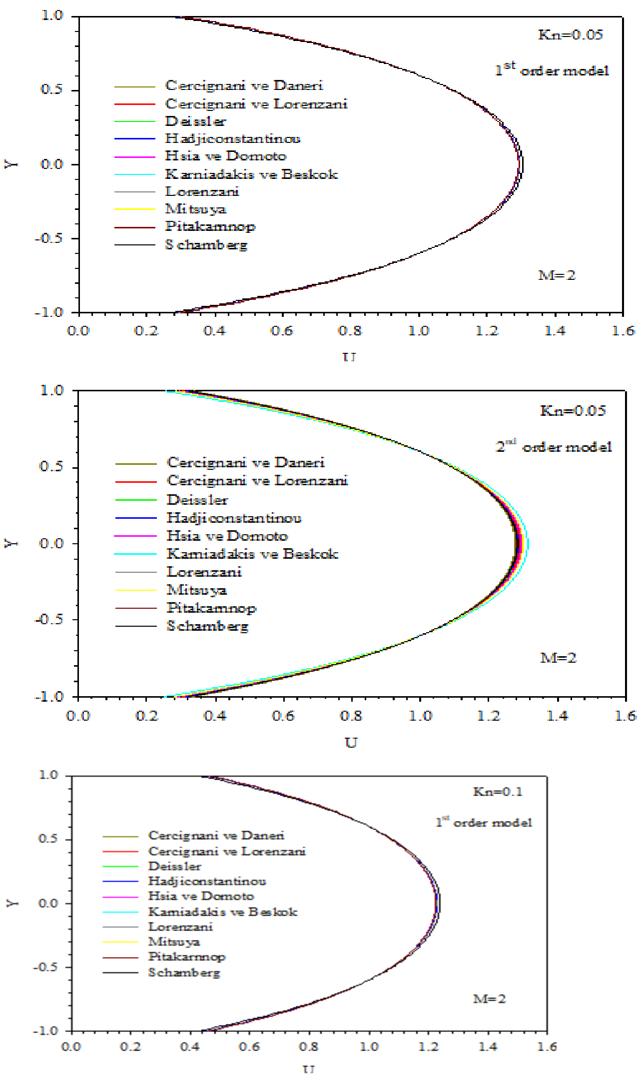

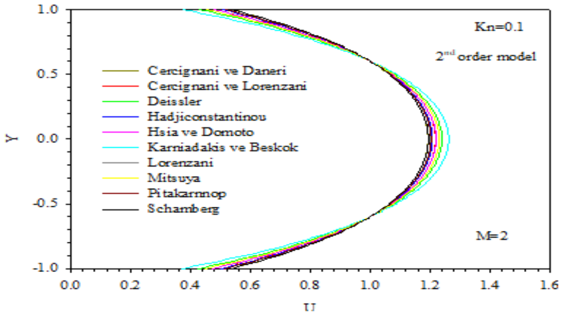

Figure 4. The impact of second order slip boundary condition coefficient for various slip models on fully developed velocity profile (M= 2).

Table 2. Comparison of slip velocities occurring in the axis at different values of Kn number and M.

Kn	M = 0									
	First order									
	[1] Y=0	[2] Y=0	[3] Y=0	[4] Y=0	[5] Y=0	[6] Y=0	[7] Y=0	[8] Y=0	[9] Y=0	[10] Y=0
0.00	1.5	1.5	1.5	1.5	1.5	1.5	1.5	1.5	1.5	1.5
0.05	1.3720	1.3742	1.3846	1.3751	1.3846	1.3846	1.3729	1.3846	1.3720	1.3846
0.10	1.2962	1.2989	1.3125	1.3001	1.3125	1.3125	1.2943	1.3125	1.2962	1.3125
	Second order									
Kn	[1] Y=0	[2] Y=0	[3] Y=0	[4] Y=0	[5] Y=0	[6] Y=0	[7] Y=0	[8] Y=0	[9] Y=0	[10] Y=0
0.00	1.5	1.5	1.5	1.5	1.5	1.5	1.5	1.5	1.5	1.5
0.05	1.364	1.372	1.374	1.370	1.380	1.389	1.367	1.382	1.366	1.373
0.10	1.277	1.294	1.288	1.287	1.301	1.324	1.283	1.307	1.283	1.284

Table 3. Comparison of slip velocities occurring in the axis at different values of Kn number and M.

Kn	M = 1									
	First order									
	[1] Y=0	[2] Y=0	[3] Y=0	[4] Y=0	[5] Y=0	[6] Y=0	[7] Y=0	[8] Y=0	[9] Y=0	[10] Y=0
0.00	1.476	1.476	1.476	1.476	1.476	1.476	1.476	1.476	1.476	1.476
0.05	1.348	1.350	1.360	1.351	1.360	1.360	1.349	1.360	1.348	1.360
0.10	1.274	1.277	1.290	1.278	1.290	1.290	1.275	1.290	1.274	1.256
	Second order									
Kn	[1] Y=0	[2] Y=0	[3] Y=0	[4] Y=0	[5] Y=0	[6] Y=0	[7] Y=0	[8] Y=0	[9] Y=0	[10] Y=0
0.00	1.476	1.476	1.476	1.476	1.476	1.476	1.476	1.476	1.476	1.476
0.05	1.338	1.348	1.348	1.345	1.355	1.366	1.342	1.358	1.341	1.346
0.10	1.251	1.271	1.260	1.262	1.276	1.306	1.258	1.284	1.258	1.256

Table 4. Comparison of slip velocities occurring in the axis at different values of Kn number and M.

Kn	M= 2									
	First order									
	[1] Y=0	[2] Y=0	[3] Y=0	[4] Y=0	[5] Y=0	[6] Y=0	[7] Y=0	[8] Y=0	[9] Y=0	[10] Y=0
0.00	1.417	1.417	1.417	1.417	1.417	1.417	1.417	1.417	1.417	1.417
0.05	1.292	1.294	1.304	1.295	1.304	1.304	1.293	1.304	1.292	1.304
0.10	1.225	1.227	1.239	1.228	1.239	1.239	1.226	1.239	1.225	1.239
	Second order									
Kn	[1] Y=0	[2] Y=0	[3] Y=0	[4] Y=0	[5] Y=0	[6] Y=0	[7] Y=0	[8] Y=0	[9] Y=0	[10] Y=0
0.00	1.417	1.417	1.417	1.417	1.417	1.417	1.417	1.417	1.417	1.417
0.05	1.277	1.290	1.286	1.285	1.295	1.313	1.282	1.300	1.282	1.283
0.10	1.193	1.218	1.239	1.207	1.219	1.262	1.202	1.230	1.203	1.194

Table 5. Comparison of slip velocities in the wall at different Kn numbers and M values.

Kn	M = 0									
	First order									
	[1] Y=±1	[2] Y=±1	[3] Y=±1	[4] Y=±1	[5] Y=±1	[6] Y=±1	[7] Y=±1	[8] Y=±1	[9] Y=±1	[10] Y=±1
0.00	0	0	0	0	0	0	0	0	0	0
0.05	0.255	0.251	0.230	0.249	0.230	0.230	0.254	0.230	0.255	0.230
0.10	0.407	0.402	0.375	0.399	0.375	0.375	0.405	0.375	0.407	0.375
	Second order									
Kn	[1] Y=±1	[2] Y=±1	[3] Y=±1	[4] Y=±1	[5] Y=±1	[6] Y=±1	[7] Y=±1	[8] Y=±1	[9] Y=±1	[10] Y=±1
0.00	0	0	0	0	0	0	0	0	0	0
0.05	0.271	0.255	0.250	0.260	0.239	0.221	0.265	0.234	0.266	0.253
0.10	0.446	0.412	0.423	0.425	0.397	0.350	0.433	0.385	0.433	0.430

Table 6. Comparison of slip velocities in the wall at different Kn numbers and M values.

Kn	M=1									
	First order									
	[1] Y=±1	[2] Y=±1	[3] Y=±1	[4] Y=±1	[5] Y=±1	[6] Y=±1	[7] Y=±1	[8] Y=±1	[9] Y=±1	[10] Y=±1
0.00	0	0	0	0	0	0	0	0	0	0
0.05	0.268	0.263	0.242	0.261	0.242	0.242	0.266	0.242	0.268	0.242
0.10	0.422	0.417	0.389	0.414	0.389	0.389	0.420	0.389	0.422	0.461
	Second order									
Kn	[1] Y=±1	[2] Y=±1	[3] Y=±1	[4] Y=±1	[5] Y=±1	[6] Y=±1	[7] Y=±1	[8] Y=±1	[9] Y=±1	[10] Y=±1
0.00	0	0	0	0	0	0	0	0	0	0
0.05	0.289	0.269	0.268	0.275	0.254	0.229	0.281	0.247	0.282	0.272
0.10	0.472	0.430	0.452	0.448	0.419	0.356	0.457	0.403	0.456	0.461

Table 7. Comparison of slip velocities in the wall at different Kn numbers and M values.

Kn	M = 2									
	First order									
	[1] Y=±1	[2] Y=±1	[3] Y=±1	[4] Y=±1	[5] Y=±1	[6] Y=±1	[7] Y=±1	[8] Y=±1	[9] Y=±1	[10] Y=±1
0.00	0	0	0	0	0	0	0	0	0	0
0.05	0.299	0.294	0.271	0.292	0.271	0.271	0.297	0.271	0.299	0.271
0.10	0.460	0.454	0.426	0.452	0.426	0.426	0.458	0.426	0.460	0.426
Kn	Second order									
	[1] Y=±1	[2] Y=±1	[3] Y=±1	[4] Y=±1	[5] Y=±1	[6] Y=±1	[7] Y=±1	[8] Y=±1	[9] Y=±1	[10] Y=±1
0.00	0	0	0	0	0	0	0	0	0	0
0.05	0.334	0.303	0.314	0.315	0.291	0.250	0.322	0.280	0.322	0.321
0.10	0.535	0.475	0.426	0.503	0.473	0.371	0.514	0.448	0.513	0.534

Table 8. Relative percentage changes of velocity depending on different Kn numbers and M values.

Kn	M = 0									
	$\frac{U_{second\ order}-U_{first\ order}}{U_{second\ order}}x100$									
	[1] Y=0	[2] Y=0	[3] Y=0	[4] Y=0	[5] Y=0	[6] Y=0	[7] Y=0	[8] Y=0	[9] Y=0	[10] Y=0
0.00	-	-	-	-	-	-	-	-	-	-
0.05	-0.57	-0.145	-0.705	-0.372	-0.318	0.323	-0.416	-0.137	-0.387	-0.822
0.10	-1.71	-0.378	-1.886	-0.978	-0.868	0.920	-1.090	-0.390	-1.013	-2.171

Table 9. Relative percentage changes of velocity depending on different Kn numbers and M values.

Kn	M = 1									
	$\frac{U_{second\ order}-U_{first\ order}}{U_{second\ order}}x100$									
	[1] Y=0	[2] Y=0	[3] Y=0	[4] Y=0	[5] Y=0	[6] Y=0	[7] Y=0	[8] Y=0	[9] Y=0	[10] Y=0
0.00	-	-	-	-	-	-	-	-	-	-
0.05	-0.762	-0.185	-0.919	-0.483	-0.413	0.431	-0.543	-0.184	-0.506	-1.069
0.10	-1.894	-0.487	-2.359	-1.243	-1.112	1.201	-1.382	-0.506	-1.287	-0.000

Table 10. Relative percentage changes of velocity depending on different Kn numbers and M values.

Kn	M = 2									
	$\frac{U_{second\ order}-U_{first\ order}}{U_{second\ order}}x100$									
	[1] Y=0	[2] Y=0	[3] Y=0	[4] Y=0	[5] Y=0	[6] Y=0	[7] Y=0	[8] Y=0	[9] Y=0	[10] Y=0
0.00	-	-	-	-	-	-	-	-	-	-
0.05	-1.150	-0.286	-1.407	-0.746	-0.640	0.670	-0.826	-0.292	-0.771	-1.628
0.10	-2.638	-0.705	0.000	-1.764	-1.598	1.837	-1.954	-0.739	-1.819	-3.767

Table 11. Relative percentage changes of velocity depending on different Kn numbers and M values.

Kn	M = 0									
	$\frac{U_{second\ order}-U_{first\ order}}{U_{second\ order}}x100$									
	[1] Y=±1	[2] Y=±1	[3] Y=±1	[4] Y=±1	[5] Y=±1	[6] Y=±1	[7] Y=±1	[8] Y=±1	[9] Y=±1	[10] Y=±1
0.00	-	-	-	-	-	-	-	-	-	-
0.05	5.809	1.564	7.753	3.923	3.632	-4.057	4.290	1.661	3.977	8.882
0.10	8.609	2.402	11.473	5.929	5.684	-6.959	6.459	2.647	5.996	12.972

Table 12. Relative percentage changes of velocity depending on different Kn numbers and M values.

Kn	M= 1									
	$\frac{U_{second\ order}-U_{first\ order}}{U_{second\ order}}x100$									
	[1] Y=±1	[2] Y=±1	[3] Y=±1	[4] Y=±1	[5] Y=±1	[6] Y=±1	[7] Y=±1	[8] Y=±1	[9] Y=±1	[10] Y=±1
0.00	-	-	-	-	-	-	-	-	-	-
0.05	7.360	1.970	9.765	4.972	4.685	-5.306	5.431	2.142	5.030	11.123
0.10	10.537	3.043	13.932	7.388	7.079	-9.218	7.983	3.371	7.463	0.000

Table 13. Relative percentage changes of velocity depending on different Kn numbers and M values.

Kn	M = 2									
	$\frac{U_{second\ order}-U_{first\ order}}{U_{second\ order}}x100$									
	[1] Y=±1	[2] Y=±1	[3] Y=±1	[4] Y=±1	[5] Y=±1	[6] Y=±1	[7] Y=±1	[8] Y=±1	[9] Y=±1	[10] Y=±x
0.00	-	-	-	-	-	-	-	-	-	-
0.05	10.529	2.934	13.763	7.233	6.833	-8.43	7.871	3.210	7.342	15.561
0.10	14.069	4.352	0.000	10.164	9.843	-15.0	10.940	4.838	10.233	20.164

4. Conclusions and Recommendations

In the study, velocity distribution was obtained analytically depending on magnetic field parameter M, first and second order slip velocity boundary condition coefficients b_1, b_2 and Knudsen number. The research is based on slip velocity boundary condition coefficients proposed for second order velocity slip boundary condition models by [1], [2], [3], [4], [5], [6], [7], [8], [9] and [10] as shown in Table 1. The results obtained for Knudsen number range between 0 and 0.1 whereas they scale between 0 and 2 for magnetic field parameter referred as Hartmann number. Slip velocity is analytically solved to accumulate Knudsen number depending on the coefficients of first and second order slip boundary conditions b_1 and b_2 as well as the magnetic field parameter M.

Using the second order slip boundary condition coefficient, it is revealed that slip velocity at M = 0 and Kn = 0 in the first and second order slip velocity boundary conditions generate a non-slip state both on the wall and axis. At M = 0, compared to the first order slip boundary condition, as the Knudsen nu is increased by the second order slip boundary condition, slip velocity on the plate wall also rises for all models except Model [6] while a lowered effect is seen in axis velocity (maximum velocity) varying by the mass position. Furthermore, slip velocity on the wall is much more increased by arising Knudsen number and magnetic field parameter M in a contradictory effect to the reduced axis velocity. The second order slip boundary condition accentuates this effect even more for all models excluding Model [6] while making velocity profile more massive (flattened) and causing a larger increase in velocity on the wall than does the first order slip velocity boundary condition.

For models [1,2,4,5,7-10], the magnetic field fosters a reducing effect on wall slip velocity whereas an enhancing impact on the axis. The magnetic field is remarked to bring out a reverse situation for model [6] with an increasing slip velocity on the axis and decreasing one on the wall. Yet, no change is noted for model [3].

5. Acknowledge

[1] Cercignani, C. and A. Daneri, Flow of a rarefied gas between two parallel plates. Journal of Applied Physics, 1963. 34(12): p. 3509-3513.

[2] Cercignani, C. and S. Lorenzani, Variational derivation of second-order slip coefficients on the basis of the Boltzmann equation for hard-sphere molecules. Physics of Fluids, 2010. 22(6): p. 062004.

[3] Deissler, R., An analysis of second-order slip flow and temperature-jump boundary conditions for rarefied gases. International Journal of Heat and Mass Transfer, 1964. 7(6): p. 681-694.

[4] Hadjiconstantinou, N.G., Comment on Cercignani's second-order slip coefficient. Physics of Fluids, 2003. 15(8): p. 2352-2354.

[5] Hsia, Y.-T. and G. Domoto, An experimental investigation of molecular rarefaction effects in gas lubricated bearings at ultra-low clearances. 1983.

[6] Karniadakis, G.E., A. Beskok, and M. Gad-el-Hak, Micro flows: fundamentals and simulation. Appl. Mech. Rev., 2002. 55(4): p. B76-B76.

[7] Lorenzani, S., Higher order slip according to the linearized Boltzmann equation with general boundary conditions. Philosophical Transactions of the Royal Society A: Mathematical, Physical and Engineering Sciences, 2011. 369(1944): p. 2228-2236.

[8] Mitsuya, Y., Modified Reynolds equation for ultra-thin film gas lubrication using 1.5-order slip-flow model and considering surface accommodation coefficient. 1993.

[9] Pitakarnnop, J., et al., A novel experimental setup for gas microflows. Microfluidics and Nanofluidics, 2010. 8(1): p. 57-72.

[10] Schamberg, R., The fundamental differential equations and the boundary conditions for high speed slip-flow, and their application to several specific problems. 1947, California institute of technology.

[11] Hartmann, J. and F. Lazarus, Hg-dynamics II. Theory of laminar flow of electrically conductive Liquids in a Homogeneous Magnetic Field, 1937. 15(7).

[12] Kushwaha, H.M. and S. Sahu, Analysis of gaseous flow in a micropipe with second order velocity slip and temperature jump boundary conditions. Heat and Mass Transfer, 2014. 50(12): p. 1649-1659.

[13] Wu, L., A slip model for rarefied gas flows at arbitrary Knudsen number. Applied Physics Letters, 2008. 93(25): p. 253103.

[14] Singh, G. and A. Chamkha, Dual solutions for second-order slip flow and heat transfer on a vertical permeable shrinking sheet. Ain Shams Engineering Journal, 2013. 4(4): p. 911-917.

[15] Yazdi, M., et al., Slip MHD liquid flow and heat transfer over non-linear permeable stretching surface with chemical reaction. International Journal of Heat and Mass Transfer, 2011. 54(15-16): p. 3214-3225.

[16] Colin, S., P. Lalonde, and R. Caen, Validation of a second-order slip flow model in rectangular microchannels. Heat transfer engineering, 2004. 25(3): p. 23-30.

[17] Rahimi, B. and H. Niazmand, Effects of high-order slip/jump, thermal creep, and variable thermophysical properties on natural convection in microchannels with constant wall heat fluxes. Heat transfer engineering, 2014. 35(18): p. 1528-1538.

[18] Roşca, A.V. and I. Pop, Flow and heat transfer over a vertical permeable stretching/shrinking sheet with a second order slip. International Journal of Heat and Mass Transfer, 2013. 60: p. 355-364.

[19] Roşca, N.C. and I. Pop, Mixed convection stagnation point flow past a vertical flat plate with a second order slip: heat flux case. International Journal of Heat and Mass Transfer, 2013. 65: p. 102-109.

[20] Turkyilmazoglu, M., Heat and mass transfer of MHD second order slip flow. Computers & Fluids, 2013. 71: p. 426-434.

[21] Aman, S., Q. Al-Mdallal, and I. Khan, Heat transfer and second order slip effect on MHD flow of fractional Maxwell fluid in a porous medium. Journal of King Saud University-Science, 2020. 32(1): p. 450-458.

[22] Liu, Y. and B. Guo, Effects of second-order slip on the flow of a fractional Maxwell MHD fluid. Journal of the Association of Arab Universities for Basic and Applied Sciences, 2017. 24: p. 232-241.

[23] Majeed, A., et al., Impact of magnetic field and second-order slip flow of Casson liquid with heat transfer subject to suction/injection and convective boundary condition. Journal of Magnetics, 2019. 24(1): p. 81-89.

[24] Qayyum, S., et al., Modeling and theoretical investigation of curved parabolized surface of second-order velocity slip flow: Combined analysis of entropy generation and activation energy. Modern Physics Letters B, 2020. 34(33): p. 2050383.

[25] Almutairi, F., S. Khaled, and A. Ebaid, MHD flow of nanofluid with homogeneous-heterogeneous reactions in a porous medium under the influence of second-order velocity slip. Mathematics, 2019. 7(3): p. 220.

[26] Sayyed, S., B. Singh, and N. Bano, MHD Stagnation-Point Dissipative Flow in a Porous Medium with Joule Heating and Second-Order Slip, in Computing, Communication and Signal Processing. 2019, Springer. p. 601-609.